International Journal of Impact Engineering 98 (2016) 1–12

Contents lists available at ScienceDirect

International Journal of Impact Engineering

journal homepage: www.elsevier.com/locate/ijimpeng

Polyurea coated aluminum plates under hydrodynamic loading: Does side matter?

O. Rijensky, D. Rittel *

Faculty of Mechanical Engineering, Technion- Israel Institute of Technology, 32000 Haifa, Israel

ARTICLE INFO

Article history:
Received 29 January 2016
Received in revised form 29 July 2016
Accepted 30 July 2016
Available online 3 August 2016

Keywords:
Cavitation
Hydrodynamic
Wave slamming
Polyurea coating
Digital image correlation

ABSTRACT

We report on the dynamic behavior of a polyurea-coated 6061 aluminum plate under hydrodynamic loading condition. The plate's deflection was measured using ultra-fast stereoscopic photography, and analyzed using 3D-DIC (digital image correlation) technique. The residual deformation of the plate after several shocks was measured using conventional cameras and the DIC technique. The experimental results show the benefits of the polyurea coating, with a clear indication that polyurea will better mitigate the shock if positioned on the side in contact with water.

1. Introduction

Wave slamming endangers the structural integrity of planning boats [1]. The eventuality of hull breaching increases significantly with the speed of the boat, and therefore becomes of prime concern for the design of fast vessels. To decrease this risk, one must reduce the impulse inflicted to hull plates during wave slamming. A viable solution is to consider flexible boats capable of deforming during slamming. Yet, when considering the somewhat flexible structures instead of fully rigid ones, one must take into account the inherent risk associated with hull plates that are thinner than in conventional design, and are therefore prone to experience larger strains. To reduce this risk, lightweight and flexible polyurea coating of the aluminum hull plates can be considered as a means to reduce the potential breaching, keeping the vessel impervious for some time. This may perhaps impair the sailing capability of the vessel in terms of speed on one hand, but will allow its safe return to harbor on the other hand.

Polyurea has long been considered as a potential component of blast-mitigation systems.

Polyurea, which was first considered in the late 1980s as a coating layer designed to reduce corrosion damage, regained the attention of the scientific community with the work of Amirkhizi et al. [2]. Those researchers formulated a constitutive model focusing on polyurea's mechanical capabilities, namely its pressure sensitivity and visco-hyper-elasticity. The work included experiments showing the increased performance of polyurea coated metal plates. It also revealed the potential of polyurea as a protective layer increasing the survivability of structures under extreme conditions such as impact, blasts, ballistic penetration etc. This work generated a vast interest in polyurea. Sarva et al. and Yi et al. [3,4] shed some light on the microstructural origins of PU behavior. PU is a block copolymer composed of both "hard" and "soft" segments which are scattered intermittently (Fig. 1). The bi-segmented chains form a structure of soft segment matrix, with the hard segment domains scattered through it acting as a crosslink between polymer chains. Experiments were conducted to study both the quasi-static and dynamic response of polyurea to compressive loadings and show its strain rate sensitivity. The latter is explained through a glassy transition occurring in the hard segments. The glassy transition consumes energy thus conferring the PU its ability to dissipate stress waves induced by dynamic loadings.

Roland [6] studied the dynamic behavior of polyurea with respect to the effects of stoichiometry on the mechanical behavior. The dynamic behavior of polyurea under dynamic tensile load was shown with emphasis on yield strength variations due to strain rate. The experimental results of Sarva et al. and Yi et al. [3,4] with those of Ronald et al. [6] inspired other researchers to try and develop constitutive models for polyurea which can be implemented in finite elements codes. Several researchers [7–9] proposed various constitutive models capable of describing the behavior of polyurea by superposing a rate dependent visco-elastic model with hyper-elastic model describing the large deformation material behavior

* Corresponding author. Faculty of Mechanical Engineering, Technion- Israel Institute of Technology, 32000 Haifa, Israel. Fax: +972 48295711.
E-mail address: merittel@technion.ac.il (D. Rittel).

http://dx.doi.org/10.1016/j.ijimpeng.2016.07.006
0734-743X/© 2016 Elsevier Ltd. All rights reserved.

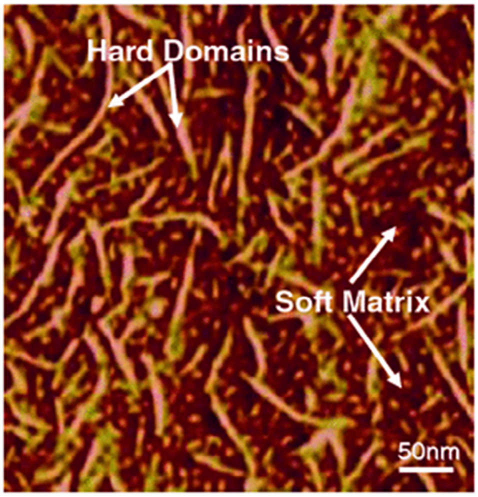

Fig. 1. AFM image of polyurea reprinted from Ref. [5].

at low strain rates. Further insights in the molecular level were suggested by Grujicic [5,10,11], discussing the physical origins of the attenuation capabilities of polyurea.

This study of the behavior of polyurea was accompanied by experimental attempts to use this material as a protective layer, increasing the survivability of structures. An effort to design sandwich structured plates as armor plates continued over the last decade or so, including it as an interlayer candidate for this purpose. Bahei-El-Din [12] proposed and studied fibrous laminates sandwich plates with a polyurea interlayer as a blast resistant structure using FE simulations.

Simulations and experiments of ballistic impact of polyurea–steel composite plates were conducted by El Sayed et al. [13] with great attention paid to developing a valid constitutive model [9]. Xue et al. compared the performance of coated vs. uncoated plated under ballistic penetration to show the energy absorption capabilities of polyurea [14]. LeBlanc et al. [15,16] and Amini et al. [17] investigated the increased capabilities of polyurea coated metal plates under hydrodynamic shocks.

It appears that in order to overcome the risks involved with wave slamming (a hydrodynamic shock), one should further explore the potential of a polyurea coating over boat's aluminum hull plates.

This experimental study examines the performance of polyurea coated vs. uncoated 6061 aluminum alloy plates. The study shows the potential of the polyurea as an active load-carrying member in case of hydrodynamic loads. It is observed that the nature of the fluid–structure interaction between the water and the tested plate affects the overall momentum history absorbed by the plate due to shocks in the water. This interaction emphasizes the importance of the *selection of the coated side of plate*. The interaction between the water and the plate takes place at their interface, and it is therefore crucial to characterize the resultant structural behavior when the hydrodynamic load encounters either the layer of (initially) soft polyurea or the tougher aluminum side. We will show that, just by flipping the coated side, one can significantly improve the performance of the hull plates. This experimental research aims at providing insights to designers and improving the efficiency of polyurea coatings for hydro-dynamically loaded structures.

The study consists of experiments aimed at simulating violent hydrodynamic loads that mimic wave slamming at high cruising speeds. First, we introduce the experimental setup and numerical model used in this work. Next, experimental results are presented; those detail the plate deflections and strains pertaining to each tested configuration. A short discussion follows, ensued by concluding remarks.

2. Experimental setup

2.1. Loading device

The experimental setup is shown schematically in Fig. 2. The test plate obturates a water-filled cylinder, the latter being shock loaded by an instrumented bar-piston system.

A compressed air gun was used to accelerate a 20 cm long, 25 mm diameter C300 Maraging steel projectile onto a 150 cm long incident bar of the same material and diameter (Hopkinson bar setup). The impact induces an elastic stress wave which propagates along the incident bar. The latter is positioned in contact with the back side of a stainless steel, 19 cm diameter, piston confined by a pressure cylinder. As the stress wave reaches the piston, it compresses the water inside the cylinder thus creating a hydrodynamic shock wave. The shock wave propagates through the water, and the pressure history is measured via a fast response pressure sensor (PCB model 113B22). It then almost immediately hits the target plate. The setup is shown in Fig. 3. Note that similar setups have been used in the past, e.g. by Deshpande et al. [18] to study the response of metallic foam cores sandwich plates under hydrodynamic shocks. Espinosa and Mori [19,20] used a similar setup with a conical pressure cylinder to study the behavior of I-core sandwich structures subjected to water blasts. In the absence of actual data from sea-experiments, the current experiments are meant to mimic the reality to some extent and the actual inflicted shocks can be adjusted at a later stage to closely replicate the sea-reality.

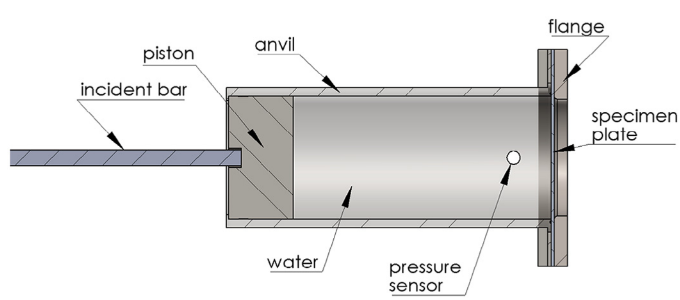

Fig. 2. Section view of the setup.

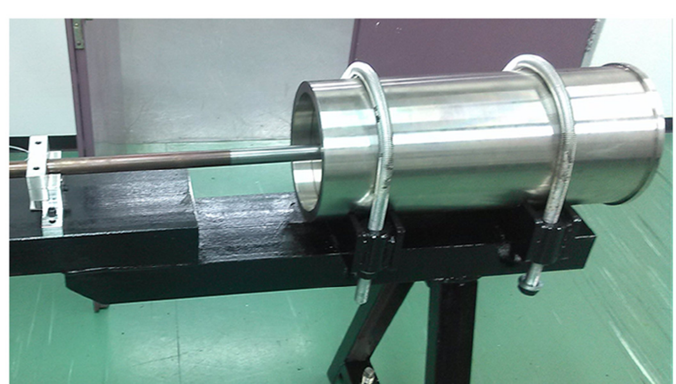

Fig. 3. Incident bar in contact with piston (inserted in the pressure cylinder).

2.2. Specimens

The hydrodynamic shock was imposed onto three 35 cm diameter, 0.8 mm thick 6061 aluminum alloy plates. The exposed part of the plate is 25 cm in diameter. The specimen plates were fastened between two flanges at the far end of the loading device by 12 screws. In order to avoid early shear failure on the periphery of the plates and make sure that the deformation accumulates at the center of the plate, the boundary conditions were changed from built in to simply support. For that purpose, the edge of the flange holding the back side of the plate was rounded to a radius of 7 mm. This radius changed the boundary condition as required and prevented unwanted early shear failure.

2.3. Photography and metrology

The deforming plate was photographed with two AVT Mako G-125B video cameras at a rate of 2 fps. Those "static" images, showing the plate between consecutive shocks, were taken with aims to measure the accumulated deflection of the plate as a result of repeated shocks.

To record the dynamic behavior of the plate, a Kirana ultra-fast camera, equipped with Loreo split lens was used. As the transient recorded pressure exceeded a threshhold of 13.5 bar, the Kirana camera was triggered to record 180 consecutive photos of the plate. We used various framing rates (50 kfps 100 kfps and 200 kfps), as those rates allowed to observe both the begininng of the deformation, i.e. the beginning of the bulging, and the induced beats and vibrations after reaching the maximum deflection (Fig. 4).

The Loreo split lens allows capturing a stereographic image with the use of a single camera (similar to the technique described in Ref. [21]). This configuration solved all issues related with camera syncing at high recording speeds.

Analysis of the photographs was conducted by using 3D-DIC technique. 3D-DIC enables the measurement of both in plane and out of plane movements in a contactless method. 2D-DIC method was invented in the 1980s [22–24] and was later developed for a 3D case using stereoscopy [25–27]. Now days, DIC has become a reliable and simple way of measurement which does not require any special light sources or cameras.

For the purpose of DIC analysis [28], a speckle pattern must be applied to the photographed surface. Due to the large size of the specimen plates (about 20 cm in diameter) and the resolution of the Kirana (about 1000 × 1000 equally divided between the two images taken) the required speckle pattern had to be relatively coarse [29,30]. Usually, such patterns are created using either an air brush or spray paint. Here, creating the larger speckles was done by manually painting them onto the photographed surface with a permanent marker. Note that hand painting with a marker reduces significantly the chipping of the paint as a result of the dynamic loads. One should note that all the speckles must be similar in size, but different in shape as much possible for the DIC software to distinguish between them. The use of permanent marker as a means to create speckle pattern should also be considered when high tensile loads are present and paint chipping becomes poses serious problems for successful DIC interpretation (Fig. 5).

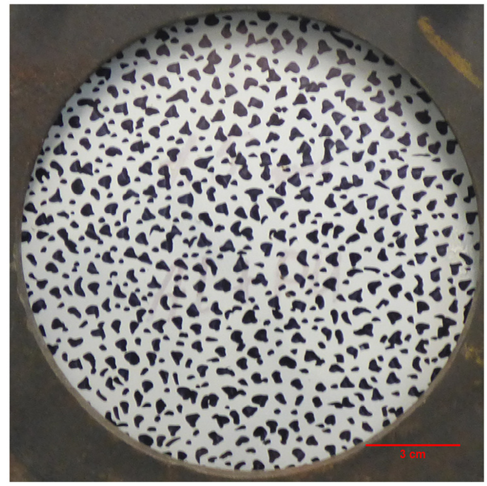

Fig. 5. Typical hand drawn speckle pattern.

The images obtained from both sets of cameras were analyzed using Match-ID 3D-DIC [31] software to measure the three dimensional full field strain and plate deflections.

3. Results

3.1. Results acquired during the deformation process

A summary of the experimental results measured after 11 consecutive shocks to each of the three specimen plates is presented in Table 1.

It should first be mentioned that none of the plates were ever breached after the first shock, irrespective of its magnitude. After applying 11 consecutive shocks to each of the three specimen plates, it was clear that they perform differently. Note that the pressure used in the compressed air gun to accelerate the projectile was kept identical throughout all 11 shots. Consequently, all the "bare" plates are deemed to have reacted identically to each shock, with the polyurea coat acting as the prime and only differentiating factor. To validate the results, the same experiment was conducted on two identical sets of specimens and the results were very much alike. For the sake of brevity, only one of the sets will be presented here.

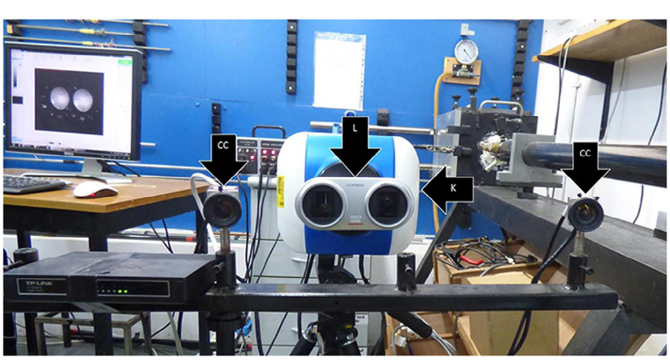

Fig. 4. Camera configuration – two conventional cameras (CC) on the sides and central ultra high speed Kirana equipped (K) with Loreo split lens (L).

Table 1
Summary of experimental results.

Specimen	Polyurea coat thickness [mm]	Aluminum thickness [mm]	Maximal deflection after 11 shots [mm]	Maximal eq. strain after 11 shots [%]	Signs of erosion
Wet PU	1.5	0.8	3	2	No
Dry PU	1.5	0.8	6	8*	Significant signs of erosion in the center
No PU	0	0.8	9	10	Small signs of erosion in the center

* Due to paint chipping at the center of the plate (where the stain reaches its maximal value) actual value is higher than the reported value.

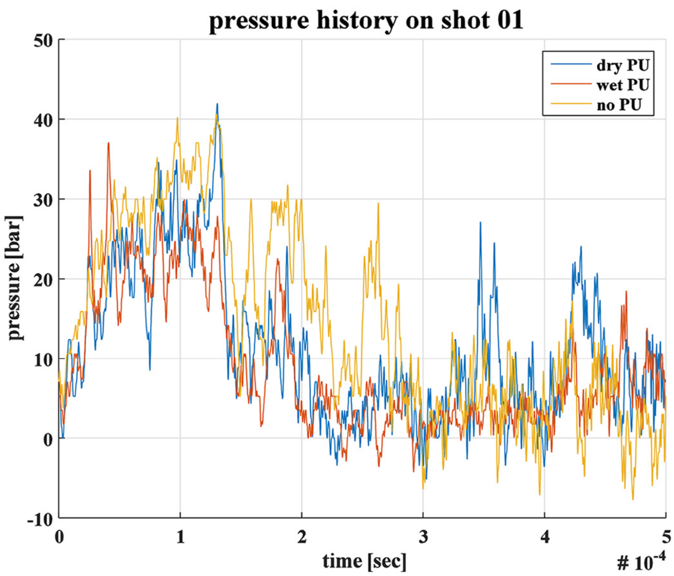

Fig. 6. Pressure history recorded through the first shot.

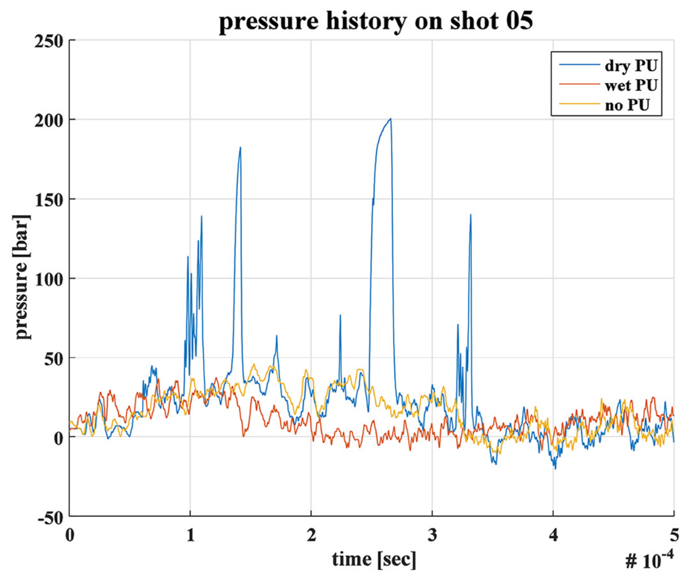

Fig. 8. Pressure history recorded through the fifth shot.

3.1.1. Pressure histories

To understand why the polyurea coat affects the behavior of the specimen plates, we will first review the pressure histories as recorded by the pressure sensor in matching shots.

In the first shot (Fig. 6), the pressure history for all three specimens seems very similar and the polyurea coat does not affect the plate behavior at all.

For the third shot (Fig. 7), a faster drop in pressure is observed with the wet PU specimen in comparison with the others. This leads to the assumption that the interaction between the polyurea and the water mitigates some of the impact energy imparted to the system. One can also notice that the duration of pressure on shot 3 is prolonged for both the dry PU and the no PU specimens, as compared with that of the first shot. This means that those plates do not bend enough to assuage to pressure wave inflicted by the water, probably due to an increase in the plates' stiffness due to prior deformations. It is important to consider the very low compressibility of water which implies that even a small deflection of the plate will increase the volume of the water in the pressure cylinder. This expansion will diminish the water pressure to zero as is allows the water to expand to the newly created free volume.

In the fifth shot (Fig. 8), one can notice high pressure spikes when PU is applied to the dry side of the plate. These spikes are apparently a first indication of water cavitation occurring in the pressure chamber. For cavitation to take place, tensile (rarefaction) waves [32] must be present and this indicates that the dry PU plate has increased its stiffness significantly due to accumulated damage. One must notice that this does not happen to the no PU specimen, and therefore *this is a direct result of the polyurea coat being located on the dry side*.

In the last shot (Fig. 9), the high pressure spikes have become very common, and it can be reasonably argued that the dry PU plate experiences a much more violent load than the other plates, under equal, thus comparable shock conditions. One can also note that the duration of the shock recorded on the wet PU plate is now also

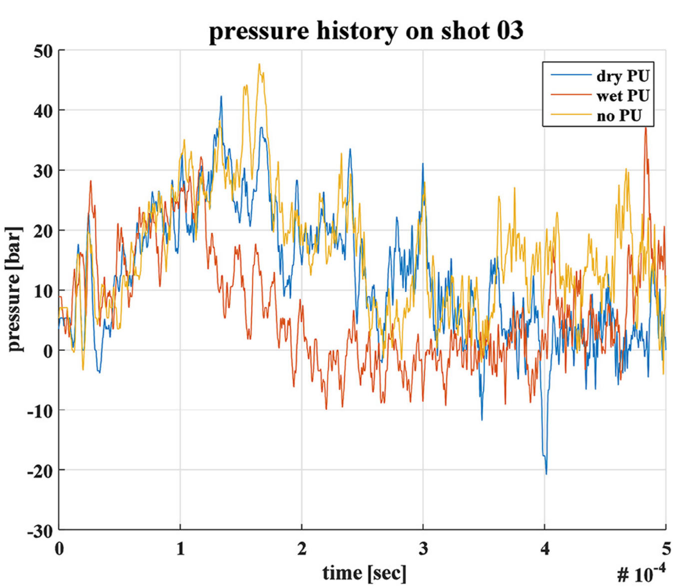

Fig. 7. Pressure history recorded through the third shot.

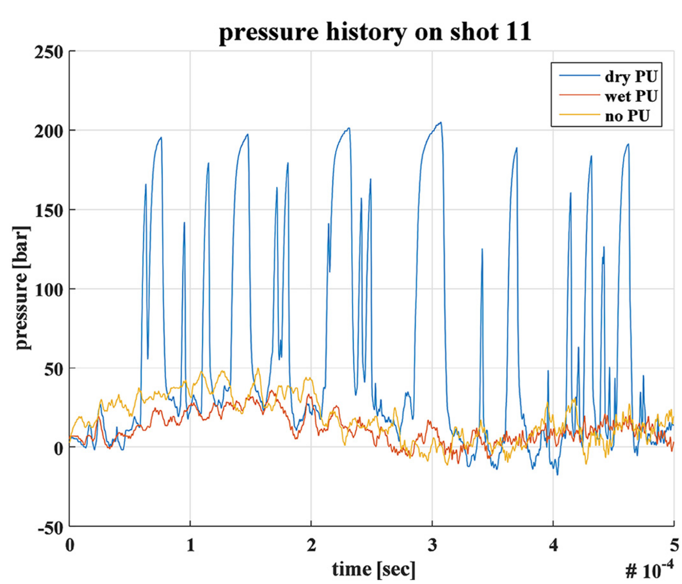

Fig. 9. Pressure history recorded through the last shot.

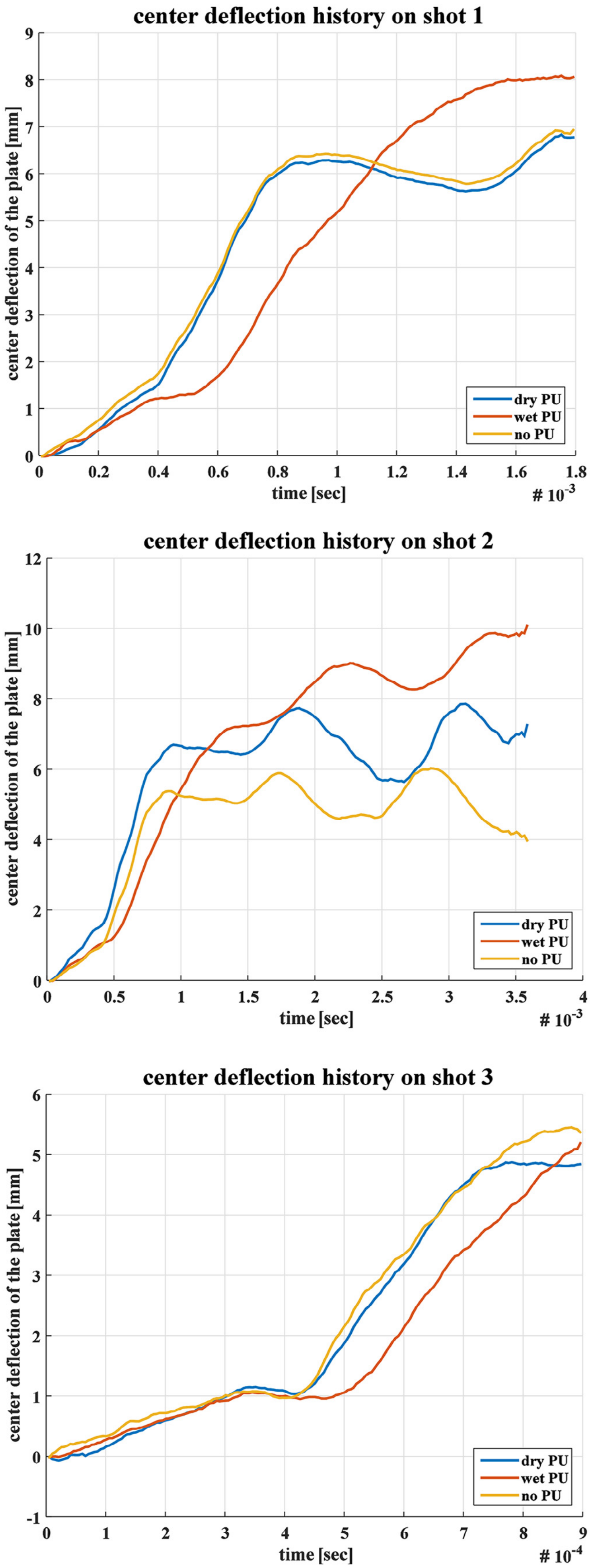

Fig. 10. Center deflection as obtained from DIC analysis for the first 3 shots.

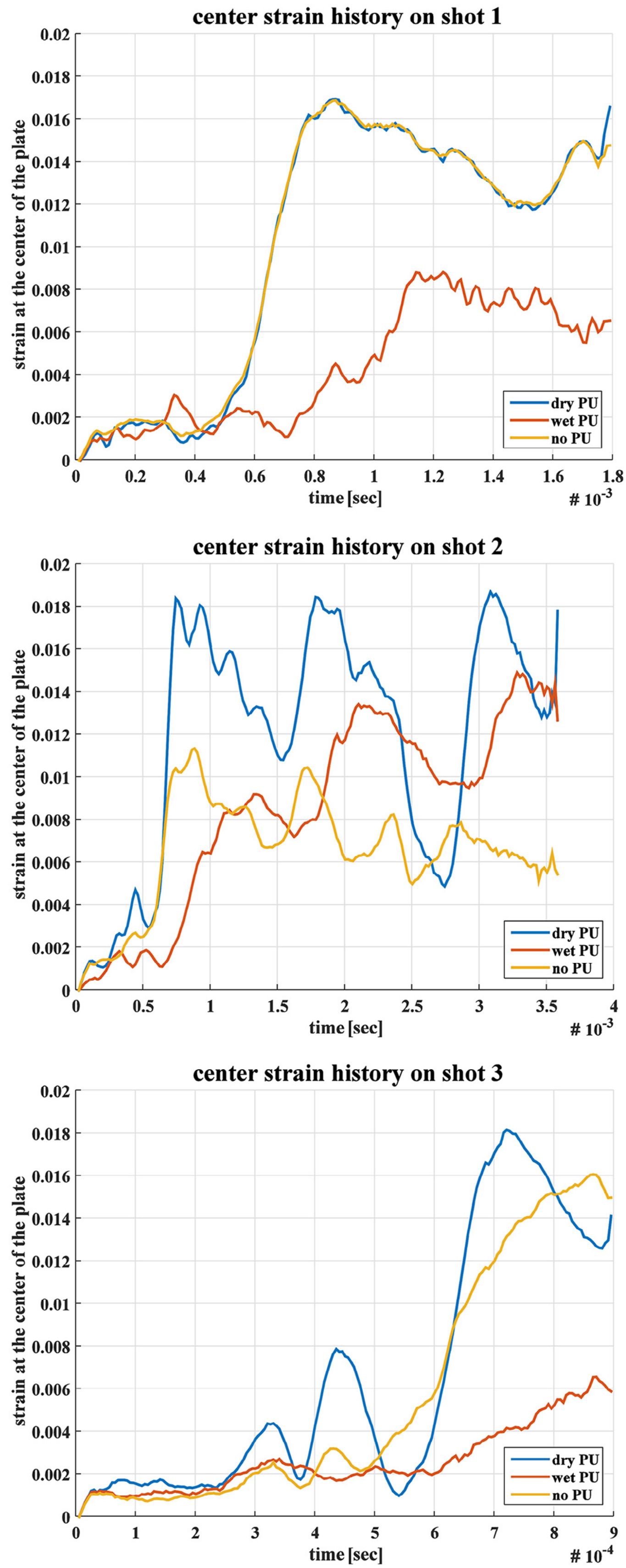

Fig. 11. Center Von Mises equivalent strain as obtained from DIC analysis through first 3 shots.

prolonged, and similar to the duration of the shocks experienced by the other 2 kinds of plates.

3.1.2. Plate deflections

The center point deflection and strain were determined from the DIC results. While looking at the graphs shown in Figs. 10 and 11, one must note they represent different shots filmed a different framing rates and therefore are not of equal time scales. It is also important to note that the deflections and strains presented are computed relative to the configuration of the plate before each impact. These results are not a representation of residual deformation accumulated with each impact.

The observation of the center point deflections in the first three shots (Fig. 10) reveals little to no difference in the response of the plates. The wet PU plate is responding slower but catches up and eventually reaches deflections similar to the deflections measured on the other plates. This is somewhat puzzling as our analysis of pressure histories suggests that the wet PU should deflect faster to reduce the pressure at an earlier time. It is important to notice that both the pressure history and center point deflection suggest that the load acting on the no PU plate during shot 2 was smaller compared to the others. This was clearly unwanted and unintended. The lower load impairs the validity of the experiments and that should be taken into account while deducing from the obtained results. To account for that lower load, we will restrict our analysis of the dynamical behavior of the plates to the first shot alone.

All in all, this comparably lower load on one out of eleven shots can be disregarded and results can still be compared.

Observing the corresponding midpoint strains (Fig. 11) reveals a more complete description of the situation and lifts this apparent contradiction.

While center point deflection is almost equal for all 3 specimens, the center point strain of the wet PU sample is relatively smaller. This means that the curvature of the wet PU plate might be smaller and probably more uniformly distributed than that of the other plates. In other words, the wet PU plate moves more like a rigid body than the other plates in which strains concentrate at the central region. Obviously this is a great advantage of the wet PU plate as strain concentration will increase accumulated damage in the center, with a potential for premature failure. To check that hypothesis, one must now consider the full field of displacements (Figs. 12–14) and strains (Figs. 15–17).

By comparing Figs. 12, 13 and 14, which show the plate displacements, one can notice the “slower” response of the wet PU

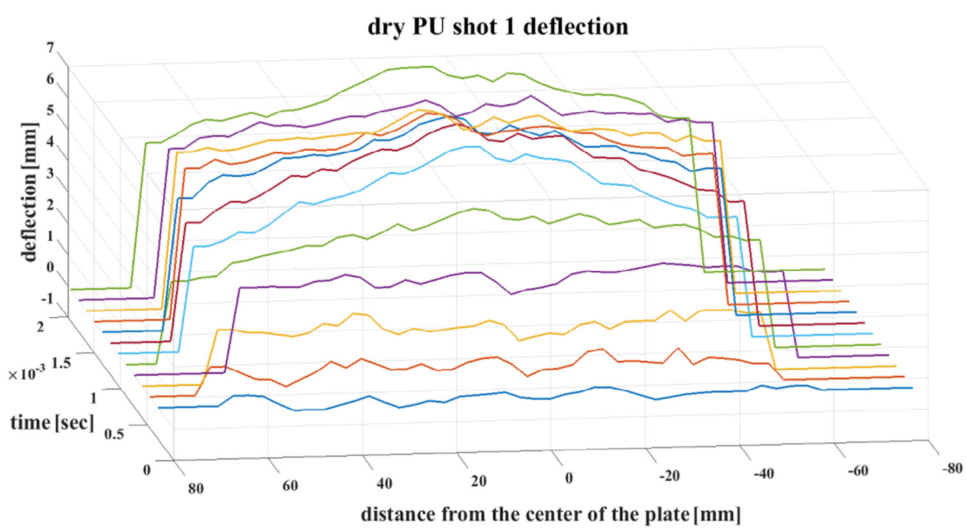

Fig. 12. History of deflections at a central cross section of the dry PU specimen plate.

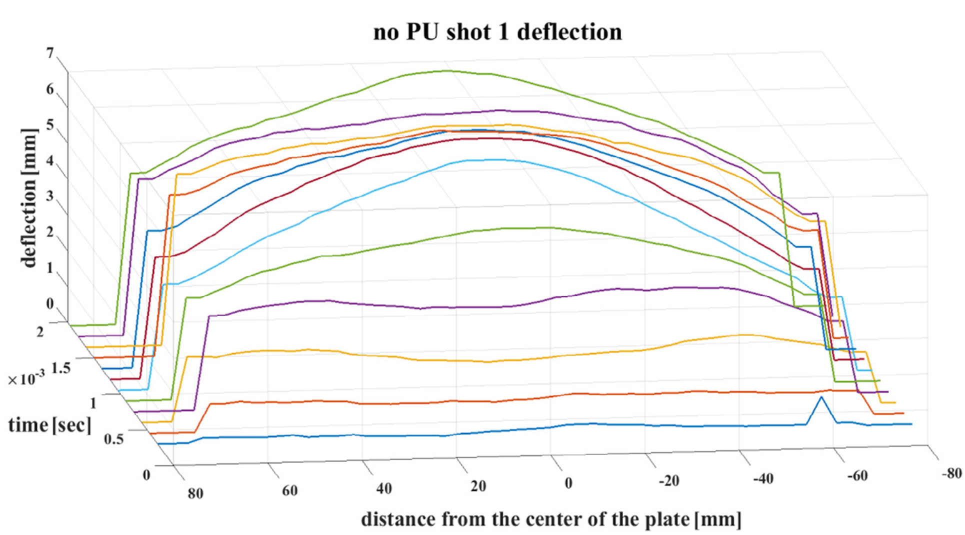

Fig. 13. History of deflections at a central cross section of the no PU specimen plate.

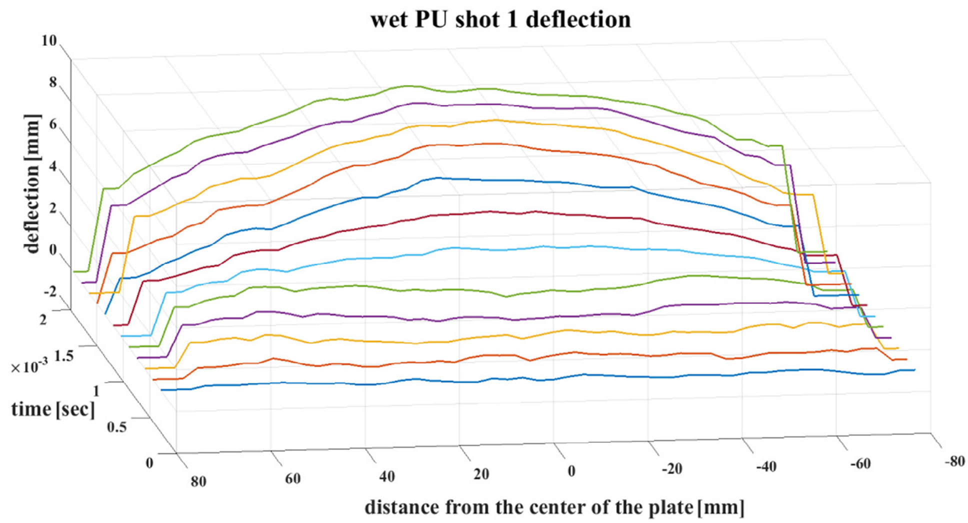

Fig. 14. History of deflections at a central cross section of the wet PU specimen plate.

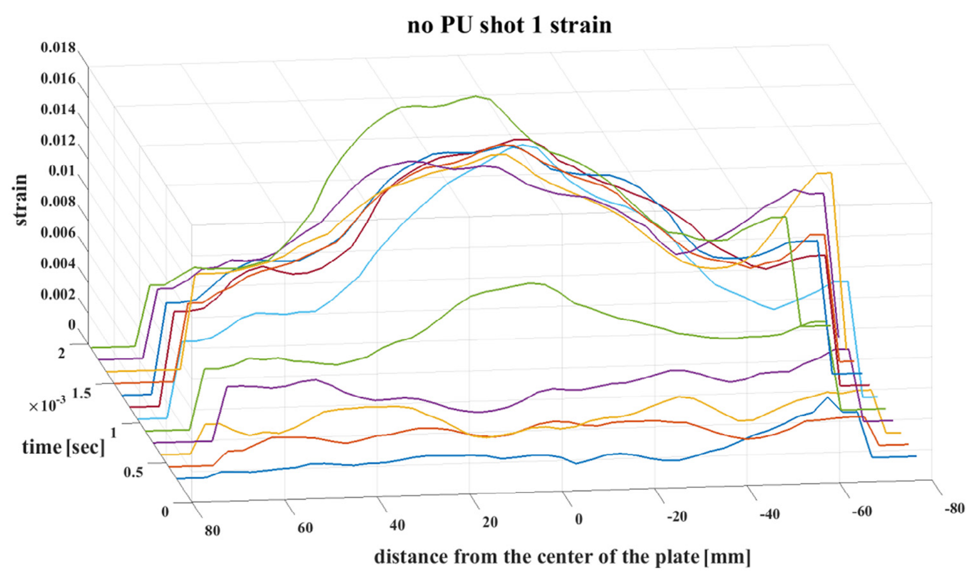

Fig. 15. Von Mises equivalent strains at a central cross section of the no PU specimen plate.

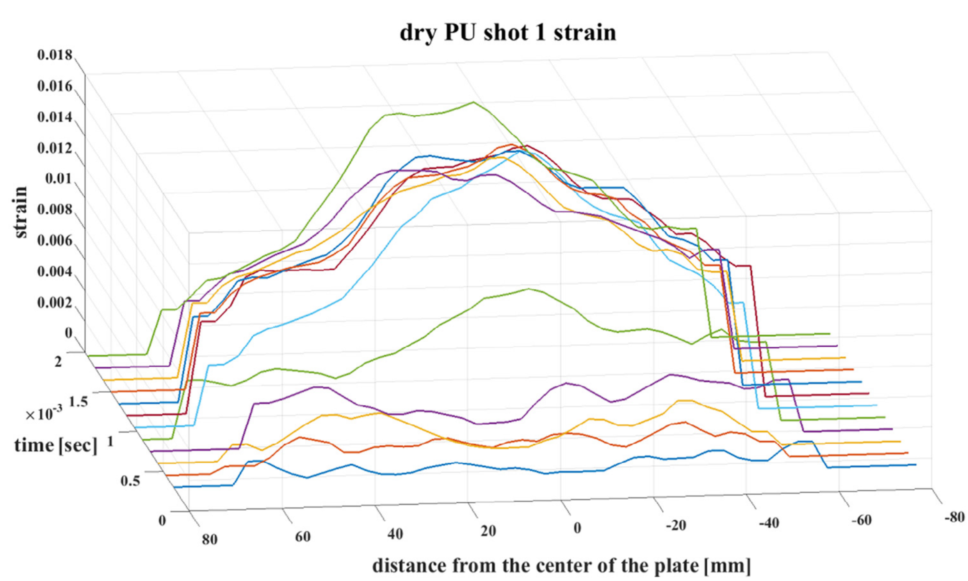

Fig. 16. Von Mises equivalent strains at a central cross section of the dry PU specimen plate.

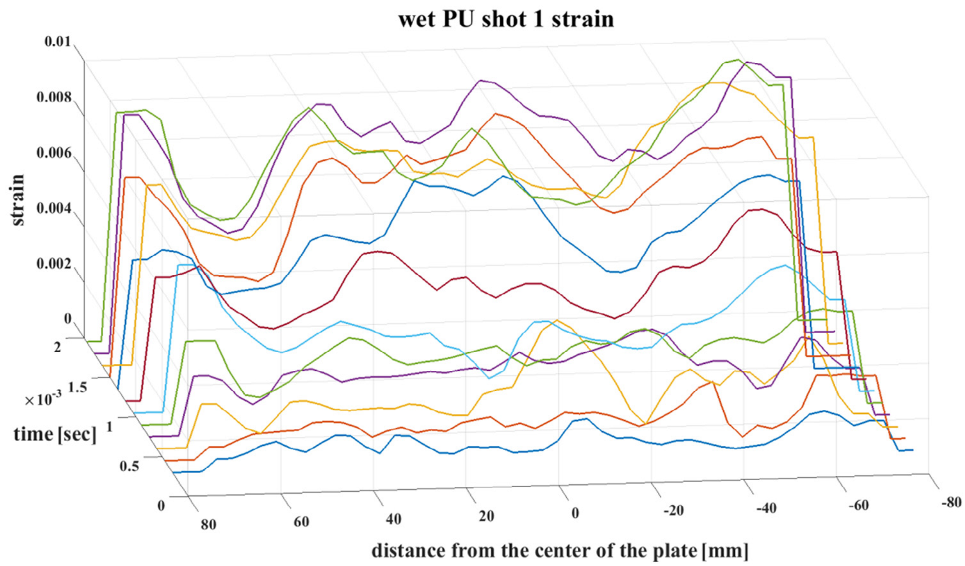

Fig. 17. Von Mises equivalent strains at a central cross section of the wet PU specimen plate.

specimen in comparison with the other plates. This comes along with the relatively smooth shape of the deflection curves for this specimen. By contrast, the other plates exhibit a larger curvature at their center with respect to the rest of the plate, a point that will be better illustrated by the full field strains. The onset of a beating motion is visible in both dry PU and no PU specimens, while the wet PU specimen behaves differently. One can notice that the wet PU specimen plate barely reaches its maximal deflection during the recorded time. The longer risetime suggests that a smaller impulse was absorbed by the wet PU plate, which can only be attributed to the "soothing" effect of the PU on the interaction between the water and the plate.

3.1.3. Plate strains

The full fields of strains are shown in Figs. 15–17. As before, the results are shown for a through-diameter cross section of the plate.

The first important thing to note is that the maximal strain in the dry PU specimen is smaller than in the other specimens. A second important observation is the strains of the dry PU and no PU specimen are clearly higher in the center than in the circumference (high curvature), while the wet PU specimen shows a more uniform distribution of strains. This supports the earlier claim of a more homogeneous strain distribution in terms of structural integrity. One can also note that with the dry PU and no PU specimens, the equivalent strain reaches its maximal value in the center very rapidly. This point to high strain rates which the polyurea is sensitive. Those high strain rates increase the stiffness of the PU dramatically, causing the structure to absorb a stronger impulse and reflect tensile waves. We consider those reflected tensile waves to be the most likely reason for cavitation occurring in the water and causing local plates erosion (Fig. 18).

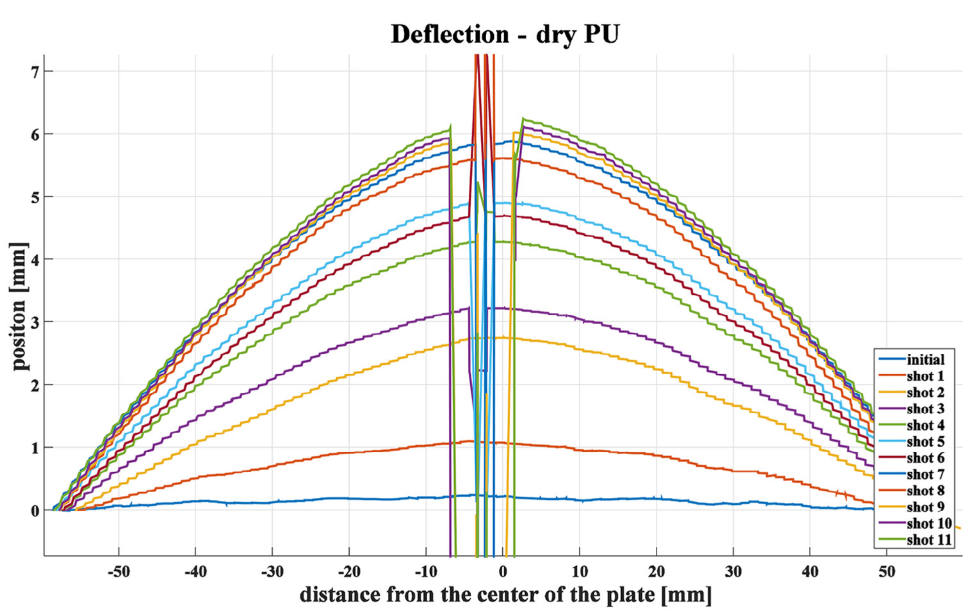

Fig. 18. Accumulated deflection of the dry PU plate.

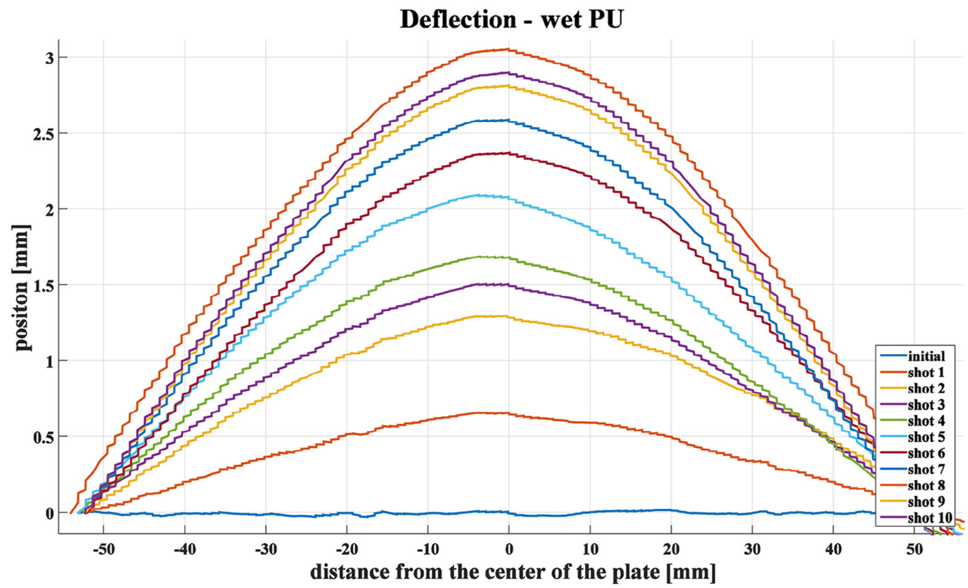

Fig. 19. Accumulated deflection of the wet PU plate.

3.2. Results acquired between consecutive shots

The accumulated deformation was also captured by conventional "slow" cameras to observe the buildup of plastic strains throughout repeated loading. It is important to note here again that the load applied to the no PU specimen during shot 2 was relatively small. But, even when ignoring shot 2 altogether, and comparing each shot of the no PU specimen with the preceding shots of other specimens, the following discussion remains valid.

We first present the accumulated deflection of all three plates (Figs. 18–20). Note the different scales of the graphs. The difference in deflections shows the ability of polyurea to mitigate the hydrodynamic shocks. Both no PU and dry PU specimens have a noisy region near the center of the plate. On the dry PU specimen, this is the result of paint chipping which altered the speckle pattern. On the no PU specimen, this is the result of the relatively large deformations. Here, as the plate deformed, the reflection of the light illuminating the plate shifted and its glare created some saturation of part of the photographic records. This could not be foreseen, since in the initial configuration, this glare was deflected far away from the camera lens.

A stronger conclusion can be derived by observing the Von Mises corresponding to the above deflections (Figs. 21–23).

We can note that the maximal Von Mises strain of both the no PU and Dry PU specimens are of similar magnitudes, even with the fact that the deflection of the no PU plate is significantly larger. In fact, if not for the paint chipping, the maximal measured Von Mises strain of the dry PU plate was probably even higher than that of the no PU plate. This occurs due to the distribution of strains. One can see the smooth distribution of strains with the wet PU plate vs. the sharp accumulation of strain near the center with the dry PU plate. This leads to the conclusion that the deformation

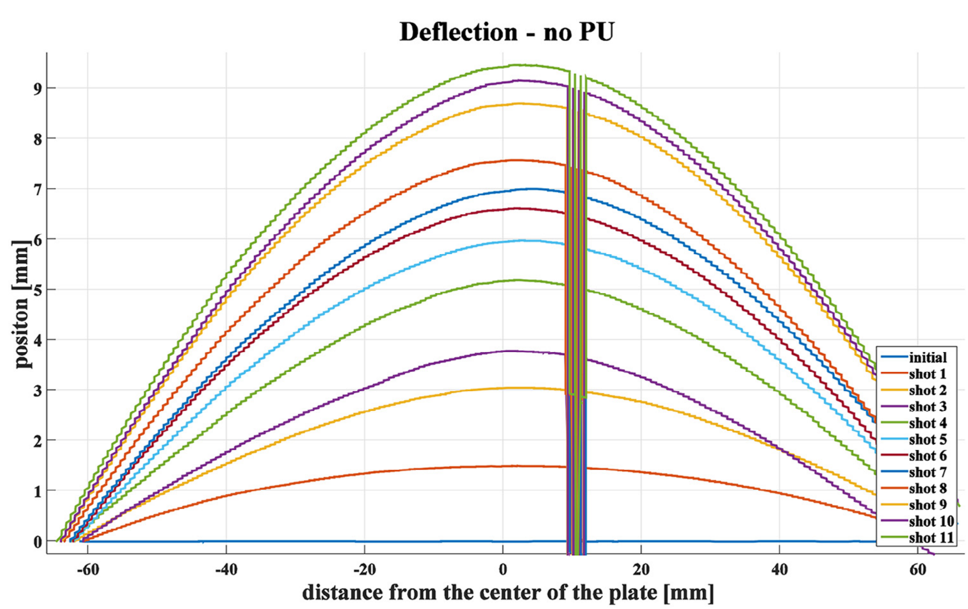

Fig. 20. Accumulated deflection of the no PU plate.

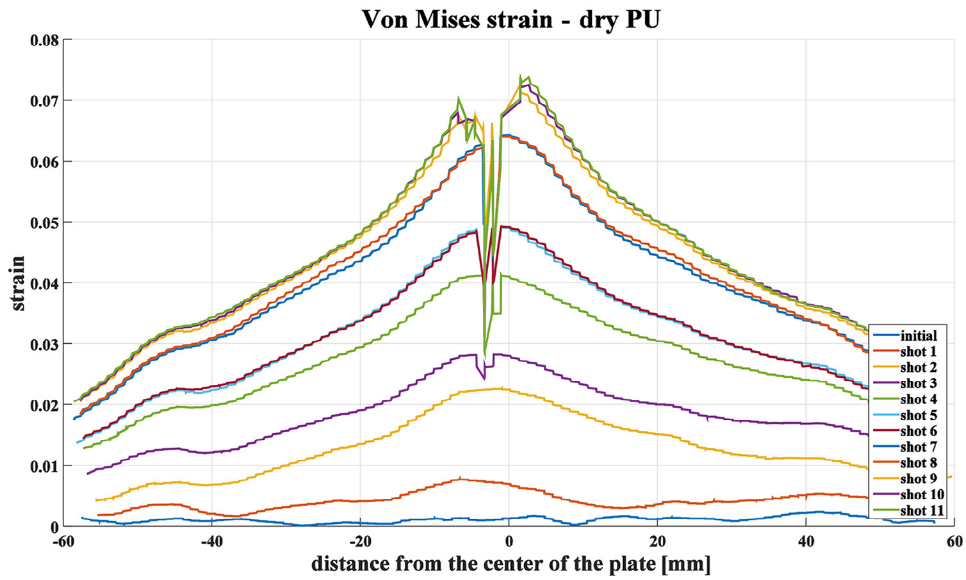

Fig. 21. Accumulated Von Mises strains of the dry PU plate.

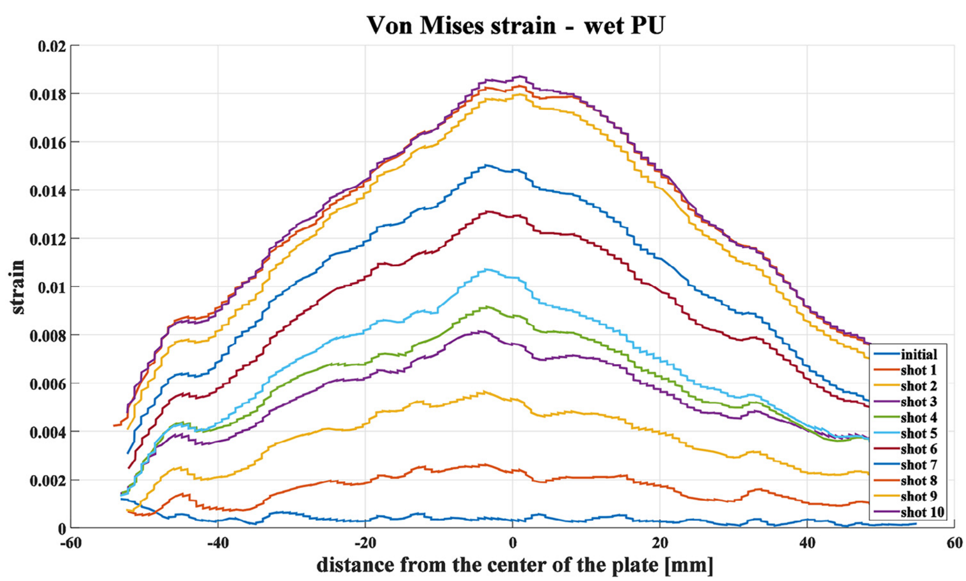

Fig. 22. Accumulated Von Mises strains of the wet PU plate.

mechanisms of the dry and wet PU plates are different. Moreover, the no PU plate deforms somewhere in between the dry and wet PU plates, as the strain distribution is neither as smooth as with wet PU nor as sharp as with the dry PU.

After removing the specimens from the setup, we observed small dents and craters in an area in the middle of the no PU and dry PU plates (Fig. 24). The worn area looks as if it was eroded by water cavitation. Together with the high pressure peaks in pressure and the paint chipping which happened on the opposite side, it seems is reasonable to assume that this damage is indeed the result of water cavitation.

If the observed damage is truly erosion due to cavitation, it clearly seems that the polyurea is an active load carrying member of the structure, as cavitation requires tensile waves, and those emerge only when a shock wave hits a stiff enough boundary (hardened polyurea). Indeed, earlier work by Amini et al. [10] reported that shocked PU can become quite stiff, to a level that compares to that of metals. The pressure spikes which are present for the dry PU specimens suggest that those are stiffer than the other two types. This can only be the result of an added stiffness coming from the shocked PU coating.

4. Summary and conclusions

The response of water-shocked polyurea coated aluminum plates was studied experimentally. The ability of the polyurea to act as load carrying member was shown, as well as the importance of the coated side of the polyurea with respect of the shock direction. The main results of the study can now be summarized as follows:

Firstly, the observed difference between the dry PU and the no PU specimens can be explained by two different reasons, namely:

- The polyurea layer increases the overall rigidity of the layered plate and therefore reduces deflections in the presence of comparable loads.
- The difference in rigidity changes the nature of the interaction with the water, giving rise to possible cavitation effects.

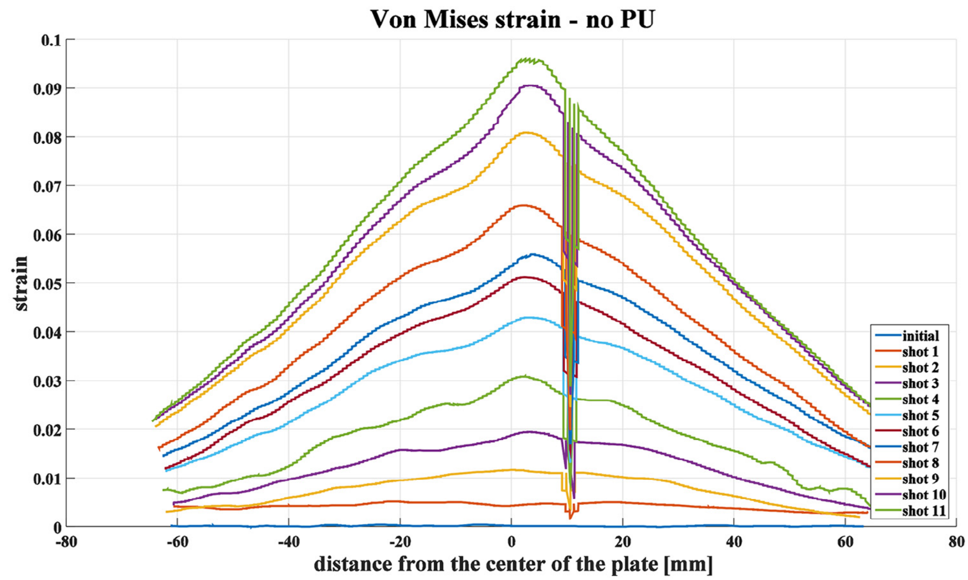

Fig. 23. Accumulated Von Mises strains of the no PU plate.

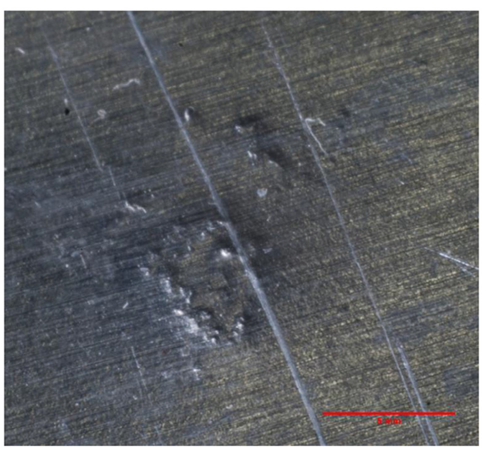

Fig. 24. Eroded, cavitation-like damage, region in the dry PU.

The wet PU plate performed better than the other 2 investigated plates as a result of the polyurea's pressure sensitivity and the apparent lack of cavitation damage.

It is therefore concluded that in the range of water pressures investigated here, the side of the coating matters with a clear advantage for the polyurea being positioned on the wet side of the plate, with all other experimental conditions kept similar.

Acknowledgments

This work is supported by the MAYMAD project under grants # 2020391 and 201809.

References

[1] Faltinsen OM, Landrini M, Greco M. Slamming in marine applications. J Eng Math 2004;48:187–217. doi:10.1023/B:engi.0000018188.68304.ae.
[2] Amirkhizi AV, Isaacs J, McGee J, Nemat-Nasser S. An experimentally-based viscoelastic constitutive model for polyurea, including pressure and temperature effects. Philos Mag 2006;86:5847–66.
[3] Yi J, Boyce MC, Lee GF Balizer E. Large deformation rate-dependent stress–strain behavior of polyurea and polyurethanes. Polymer (Guildf) 2006;47:319–29. doi:10.1016/j.polymer.2005.10.107.
[4] Sarva SS, Deschanel S, Boyce MC, Chen W. Stress–strain behavior of a polyurea and a polyurethane from low to high strain rates. Polymer (Guildf) 2007;48:2208–13. doi:10.1016/j.polymer.2007.02.058.
[5] Grujicic M, Pandurangan B, Bell WC, Cheeseman BA, Yen C-F, Randow CL. Molecular-level simulations of shock generation and propagation in polyurea. Mater Sci Eng A 2011;528:3799–808. doi:10.1016/j.msea.2011.01.081.
[6] Roland CM, Twigg JN, Vu Y, Mott PH. High strain rate mechanical behavior of polyurea. Polymer (Guildf) 2007;48:574–8. doi:10.1016/j.polymer.2006.11.051.
[7] Shim J, Mohr D. Rate dependent finite strain constitutive model of polyurea. Int J Plast 2011;27:868–86. doi:10.1016/j.ijplas.2010.10.001.
[8] Li C, Lua J. A hyper-viscoelastic constitutive model for polyurea. Mater Lett 2009;63:877–80. doi:10.1016/j.matlet.2009.01.055.
[9] El Sayed T. Constitutive models for polymers and soft biological tissues 2008.
[10] Grujicic M, Yavari R, Snipes JS, Ramaswami S, Runt J, Tarter J, et al. Molecular-level computational investigation of shock-wave mitigation capability of polyurea. J Mater Sci 2012;47:8197–215. doi:10.1007/s10853-012-6716-4.
[11] Grujicic M, Snipes JS, Ramaswami S, Yavari R, Ramasubramanian MK. Meso-scale computational investigation of shock-wave attenuation by trailing release wave in different grades of polyurea. J Mater Eng Perform 2013;doi:10.1007/s11665-013-0760-3.
[12] Bahei-El-Din YA, Dvorak GJ, Fredricksen OJ. A blast-tolerant sandwich plate design with a polyurea interlayer. Int J Solids Struct 2006;43:7644–58. doi:10.1016/j.ijsolstr.2006.03.021.
[13] El Sayed T, Mock W, Mota A, Fraternali F, Ortiz M. Computational assessment of ballistic impact on a high strength structural steel/polyurea composite plate. Comput Mech 2008;43:525–34. doi:10.1007/s00466-008-0327-6.
[14] Xue L, Mock W, Belytschko T. Penetration of DH-36 steel plates with and without polyurea coating. Mech Mater 2010;42:981–1003. doi:10.1016/j.mechmat.2010.08.004.
[15] LeBlanc J, Gardner N, Shukla A. Effect of polyurea coatings on the response of curved E-glass/vinyl ester composite panels to underwater explosive loading. Compos Part B Eng 2013;44:565–74. doi:10.1016/j.compositesb.2012.02.038.
[16] LeBlanc J, Shillings C, Gauch E, Livolsi F, Shukla A. Near field underwater explosion response of polyurea coated composite plates. Exp Mech 2015; doi:10.1007/s11340-015-0071-8.
[17] Amini MR, Isaacs J, Nemat-Nasser S. Investigation of effect of polyurea on response of steel plates to impulsive loads in direct pressure-pulse experiments. Mech Mater 2010;42:628–39. doi:10.1016/j.mechmat.2009.09.008.
[18] Deshpande VS, Heaver A, Fleck NA. An underwater shock simulator. Proc R Soc A Math Phys Eng Sci 2006;462:1021–41. doi:10.1098/rspa.2005.1604.
[19] Espinosa HD, Lee S, Moldovan N. A novel fluid structure interaction experiment to investigate deformation of structural elements subjected to impulsive loading. Exp Mech 2006;46:805–24. doi:10.1007/s11340-006-0296-7.
[20] Mori A, Hokamoto K, Fujita M. Characteristics of the new explosive welding technique using underwater shock wave-based on numerical analysis. Mater Sci Forum 2004;465-466:307–12.
[21] Genovese K, Casaletto L, Rayas JA, Flores V, Martinez A. Stereo-Digital Image Correlation (DIC) measurements with a single camera using a biprism. Opt Lasers Eng 2013;51:278–85. doi:10.1016/j.optlaseng.2012.10.001.
[22] He ZH, Sutton MA, Ranson WF, Peters WH. Two-dimensional fluid-velocity measurements by use of digital-speckle correlation techniques. Exp Mech 1984;24:117–21. doi:10.1007/BF02324993.
[23] Chu TC, Ranson WF, Sutton MA. Applications of digital-image-correlation techniques to experimental mechanics. Exp Mech 1985;25:232–44. doi:10.1007/BF02325092.

[24] Sutton M, Wolters W, Peters W, Ranson W, McNeill S. Determination of displacements using an improved digital correlation method. Image Vis Comput 1983;1:133–9. doi:10.1016/0262-8856(83)90064-1.
[25] Cardenas-Garcia JF, Yao HG, Zheng S. 3D reconstruction of objects using stereo imaging. Opt Lasers Eng 1995;22:193–213. doi:10.1016/0143-8166(94)00046-D.
[26] Sutton MA, Yan JH, Tiwari V, Schreier HW, Orteu JJ. The effect of out-of-plane motion on 2D and 3D digital image correlation measurements. Opt Lasers Eng 2008;46:746–57. doi:10.1016/j.optlaseng.2008.05.005.
[27] Lava P, Cooreman S, Coppieters S, De Strycker M, Debruyne D. Assessment of measuring errors in DIC using deformation fields generated by plastic FEA. Opt Lasers Eng 2009;47:747–53. doi:10.1016/j.optlaseng.2009.03.007.
[28] Pan B, Qian K, Xie H, Asundi A. Two-dimensional digital image correlation for in-plane displacement and strain measurement: a review. Meas Sci Technol 2009;20:062001. doi:10.1088/0957-0233/20/6/062001.
[29] Yaofeng S, Pang JHL. Study of optimal subset size in digital image correlation of speckle pattern images. Opt Lasers Eng 2007;45:967–74. doi:10.1016/j.optlaseng.2007.01.012.
[30] Lecompte D, Smits A, Bossuyt S, Sol H, Vantomme J, Van Hemelrijck D, et al. Quality assessment of speckle patterns for digital image correlation. Opt Lasers Eng 2006;44:1132–45. doi:10.1016/j.optlaseng.2005.10.004.
[31] MatchID- Metrology Beyond Colors n.d. <http://www.matchidmbc.com>.
[32] Caupin F, Herbert E. Cavitation in water: a review. Comptes Rendus Phys 2006;7:1000–17. doi:10.1016/j.crhy.2006.10.015.